JOURNAL OF GUIDANCE, CONTROL, AND DYNAMICS
Vol. 25, No. 2, March–April 2002

Order Reduction and Closed-Loop Vibration Control in Helicopter Fuselages

Anita Mathews,* V. R. Sule,† and C. Venkatesan‡
Indian Institute of Technology, Kanpur 208 016, India

The problem of vibration reduction in helicopter fuselages using the concept of active control of structural response is addressed. When the large size of the coupled gearbox–flexible fuselage system dynamics is considered, first a balanced-realization-based order reduction is employed to reduce the size of the problem. Then using the reduced-order model, a closed-loop controller is designed to minimize the vibratory levels in the fuselage with the constraint that the controller ensures stability of the original full-order system. The controller design is based on the concept of disturbance rejection by the internal model principle. When a four-block representation of the problem and doubly coprime factorization theory is employed, a stable controller is designed for this multi-input/multi-output control problem. It is observed that this controller yields a closed-loop transfer function, which rejects the external disturbance not only at the desired frequency but also in its neighborhood. In addition, contrary to open-loop control, the present technique of closed-loop control reduces the vibratory levels both in the fuselage and the gearbox. The influence of sensor locations on vibration minimization has also been highlighted.

Nomenclature

$[A]$, $[B]$, $[C]$	=	system matrix, control matrix, and output matrix, respectively
$[A]$, $[B_1]$, $[B_2]$	=	system matrix, external disturbance matrix, and control matrix of the reduced model, respectively
$[A_b]$, $[B_{w1b}]$, $[B_{u1b}]$	=	system matrix, external disturbance matrix, and control matrix of the balanced model, respectively
$[A_f]$, $[B_w]$, $[B_u]$	=	system matrix, external disturbance matrix, and control matrix of the full-order model, respectively
C_i, C^i	=	damping of the ith gearbox mounting
$[C_y]$, $[C_z]$	=	measurement matrix and output matrix, respectively.
$[C_{y1}]$, $[C_{z1}]$	=	measurement matrix and output matrix in transformed space, respectively
$[C_{y1b}]$, $[C_{z1b}]$	=	measurement matrix and output matrix in balanced space, respectively
$[C_1]$, $[C_2]$	=	measurement matrix and output matrix in reduced space, respectively
F_c	=	control force
F_x, F_y, F_z	=	vibratory forces at hub
$G(s)$	=	transfer matrix in Laplace domain, $C(sI - A)^{-1}B$
$\{I_{xx}, I_{yy}, I_{zz}\}_F$	=	mass moment of inertia of fuselage
$\{I_{xx}, I_{yy}, I_{zz}\}_{GB}$	=	mass moment of inertia of gearbox
K	=	controller transfer function or gain matrix
K_i, K^i	=	stiffness of the ith gearbox mounting
M_x, M_y, M_z	=	vibratory moments at hub
m_B	=	rotor blade mass
m_F	=	mass of fuselage
m_{GB}	=	mass of gearbox
NB	=	number of blades in the rotor system
P	=	controllability grammian
P^*	=	controllability grammian in balanced space
$\{p\}$	=	state vector
Q	=	observability grammian
Q^*	=	observability grammian in balanced space
$\{q\}$	=	state vector in original modal space
$\{\bar{q}\}$	=	state vector in transformed space
T_{zw}	=	closed-loop transfer function relating output z and input disturbance w
$\bar{T}$, T	=	transformation matrices
U	=	orthogonal matrix
$\{u\}$	=	control input vector
$\{w\}$	=	external disturbance vector
$\{x\}$	=	state vector in reduced space
$\{x_b\}$	=	state vector in balanced space
$\{x_1\}$, $\{x_2\}$	=	controllable (flexible) and uncontrollable (rigid-body) state vectors, respectively
$\{y\}$	=	measurement vector
$\{z\}$	=	output vector
β_F	=	structural damping coefficient
σ_i	=	Hankel singular values
Ω	=	rotor angular velocity
ω_0	=	frequency of external disturbance

Received 24 January 2000; revision received 1 May 2001; accepted for publication 6 August 2001.

*Graduate Student, Department of Electrical Engineering.
†Associate Professor, Department of Electrical Engineering; currently Associate Professor, Department Electrical Engineering, Indian Institute of Technology, Bombay, 400 076, India.
‡Professor, Department of Aerospace Engineering. Senior Member AIAA.

I. Introduction

HELICOPTERS are complex dynamic systems with many rotating components. During operation, the highly flexible rotor blades undergo moderate structural deformations involving coupled flap bending, lag bending, torsion, and axial modes; in addition, they experience cyclic variation in aerodynamic loads in forward flight. The periodic variation of inertia and aerodynamic loads of the main rotor system is the major source of vibration in helicopters, and these loads increase with increase in forward speed. The vibratory rotor loads are transmitted to different parts of the fuselage through a complicated load path and cause discomfort to pilot and crew, equipment deterioration, fatigue damage to the structure, and increased maintenance cost, thereby restricting the operation and efficiency of the vehicle.

With the increasing demand for high-speed and high-performance helicopters, along with improved system reliability and reduced maintenance costs, vibration reduction has become an important design criterion. For present day helicopters, the general requirement is to have a maximum vibratory level of 0.1 g in the fuselage. However, in future, with the adoption of more stringent vibration control, it will become necessary to reduce the vibratory levels below 0.05 g or even 0.02 g (Ref. 1). Excellent reviews on vibration

and its control were presented by Reichert[2] and Loewy.[3] A detailed summary of the contributions made by NASA/U.S. Army to rotorcraft vibration technology is presented in Ref. 4.

The control schemes adopted so far to reduce vibration in helicopters can be broadly classified as either passive or active control technologies. It is well known that a major contribution to helicopter vibration is due to the main rotor. Therefore, the geometry of the rotor system and the structural dynamic characteristics of the rotor blades and fuselage play a significant role in influencing the vibration in helicopters. One of the passive methods of reducing vibrations is to design carefully the rotor hub and rotor blades.[5] Because rotor design is based on a compromise of several conflicting aeroelastic and aeromechanical stabilities, as well as performance and handling quality requirements, vibration reduction solely by a proper design of a rotor blade would be impossible. Also proper placement of fuselage natural frequencies away from the excitation frequency would be very difficult because helicopter fuselage structures have the unique characteristic of having only a small distributed structural mass in comparison to several large concentrated masses, representing engine, gearbox, rotor systems, and so on. Therefore, the fuselage structure has a high modal density, that is, many closely spaced natural frequencies, and very complex mode shapes.[6]

In general, passive vibration control schemes include hub- or blade-mounted pendulum absorbers, antiresonant vibration isolation devices such as like dynamic antiresonant vibration isolation, antiresonant isolation system (ARIS), and liquid inertia vibration eliminator, structural modifications, and structural optimization. Because passive devices are tuned to provide maximum vibration reduction at specific frequency, for any change in operating condition, their performance will degrade considerably. It is generally accepted that jet-smooth ride in helicopters would be possible in the future only with the incorporation of active control schemes.[7] Active control methodologies include higher harmonic control (HHC), individual blade control (IBC), active flap control (AFC) and active control of structural response (ACSR). Whereas HHC, IBC and AFC control schemes are aimed at reducing the blade loads in rotating frame, ACSR is employed in the nonrotating frame to cancel the effect of vibratory hub loads on the fuselage. A detailed comparison of active vibration control schemes is provided in Ref. 8.

The concept of the ACSR scheme is based on the principle of superposition of two independent responses of a linear system, such

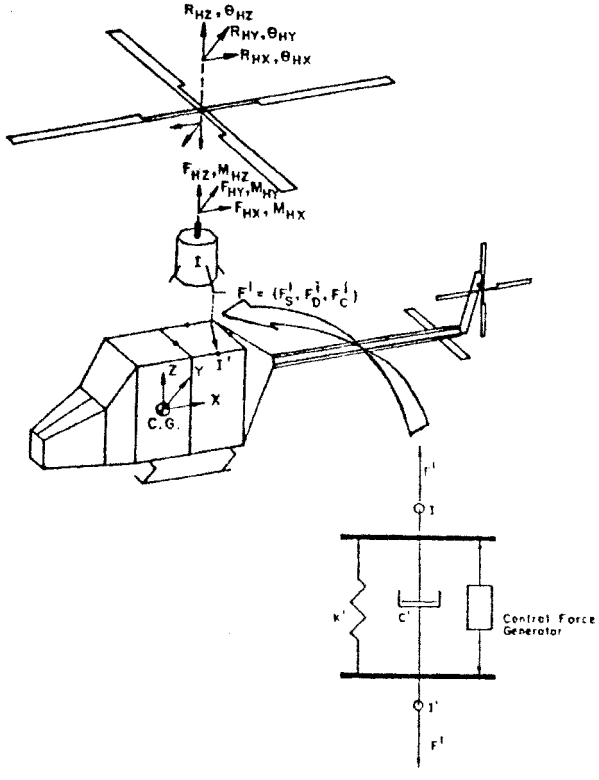

Fig. 1 Schematic of helicopter with the ACSR scheme.

that the total response is zero (Refs. 9 and 10). A schematic of a helicopter with ACSR is shown in Fig. 1. The rotor loads are transmitted to the fuselage through the gearbox support structure. The support structure is idealized as a spring, a damper, and a control force generator. In the passive scheme, the control force generator corresponds to a vibration absorber mass (as in ARIS), whereas in the case of ACSR, the control force generator can be an electrohydraulic actuator or an electromechanical actuator or a smart piezoactuator.[7] Because of several advantages, incorporation of the ACSR scheme in helicopters is being pursued vigorously by industries.[9–11]

Some of the important aspects in practical implementation of active vibration control schemes are 1) selection of sensor location for vibration measurement, 2) selection of actuator locations, and 3) formulation of closed-loop control scheme for vibration minimization. In the case of the ACSR scheme, the actuators are placed at the gearbox support structure, whereas the sensors have to be placed at optimal locations to maximize the effect of vibration control in fuselage. Recently, in Ref. 12, a systematic mathematical procedure, employing Fisher information matrix (see Ref. 13) has been successfully applied to identify the optimal sensor locations for vibration reduction in helicopter fuselages. The reference parameters used in the selection process are the elements of a vector defined as the effective independence distribution vector and the condition number of the Fisher information matrix. It was shown in Ref. 12 that, irrespective of the excitation frequency, these optimally selected sensor locations experience high levels of vibration.

Because the frequency of the dominant component of fuselage vibration in helicopters is always NB/rev (also known as blade passage frequency), all vibration control schemes aim to minimize the NB/rev component of fuselage vibration. When the ACSR scheme of vibration reduction in fuselage was applied, the active control forces were evaluated by minimizing a cost function in Refs. 9–12. In Ref. 14, the control forces were evaluated by equating the total steady-state force across the servoactuators to zero. It is noted in Refs. 12 and 14 that, on reducing fuselage vibration, the ACSR scheme of vibration minimization increases the gearbox vibratory levels[12] and hub loads.[14] In Ref. 15, in addition to describing the methods of active control of vibration in helicopters, the authors have highlighted the applicability of internal model principle of disturbance rejection for the design of closed-loop controllers. The idea of disturbance rejection of fixed-frequency (NB/rev) signal is based on the internal model principle,[16] where a suitable duplicated model simulating the dynamic characteristics of the disturbance signal is incorporated in the feedback path. The purpose of the internal model is to provide closed-loop transmission zeros that cancel the poles of the disturbance signal.

In any dynamic analysis of complex structures, there are several stages of model order reduction, namely, 1) the distributed parameter system with infinite degrees of freedom is reduced to manageable finite element model with a few thousand degrees of freedom and 2), in the next stage using undamped free vibration modes obtained from an eigenanalysis of the finite element model, a further reduction in the model order is achieved by modal transformation with truncated number of modes (considering only the first few modes of interest). This reduced-order model is then used for response and stability analysis. In the case of helicopters, due to high modal density of the fuselage structural modes, even in the modal space a large number of modes have to be considered particularly for the vibration analysis. It is known that a dynamic model with large number of degrees of freedom will lead to numerical difficulties and high computational costs. In addition, for closed-loop compensator design, a high-order system is difficult to use, and the controller will have reduced efficiency. It is always preferable to have a low-order system for the design of the compensator, with the constraint that the controller designed for the small-order system will ensure stability when incorporated in the full-order system. (Note that in this paper full-order system implies the system in modal space.)

A technique known as model order reduction via balanced state-space representation has been developed by Moore.[17] This technique is highly suitable for large systems incorporating multivariable control. In analyzing model reduction for flexible space structure, it was shown in Ref. 18 that balanced-realization-based order reduction

is superior to modal-truncation-based order reduction particularly when the natural frequencies are closely spaced. A brief description of this technique is provided here for convenience.[19,20] A proper way to reduce the order of a dynamic system for control purposes is to delete those states that are least controllable and observable. For a systematic approach to delete the least observable and controllable states, one requires a measure of controllability and observability. It is known that the singular values of controllability and observability grammians define a measure of controllability and observability in certain directions of the state space. Because the grammians are variant under a coordinate transformation, it is shown that there exists a coordinate system in which the grammians are equal and diagonal. The corresponding space is denoted as the balanced space. A reduced-order model of the system can be obtained by deleting the least controllable and observable states in the balanced space. Then for the reduced model, a suitable controller can be designed. Of course, the efficiency of the compensator has to be established by analyzing the full-order system with the controller designed for low-order system.

The aim of this study is to address the problem of vibration minimization using the ACSR scheme in helicopter fuselages, by integrating several independent concepts in a novel manner. This is achieved by first employing balanced-realization-based order reduction and then the concept of disturbance-rejection-based closed-loop control using doubly coprime factorization theory.

The main objectives of this study follow:

1) Formulate a reduced-order model for the coupled gearbox/fuselage helicopter model using balanced realization.

2) Using the reduced-order model, design a closed-loop controller for vibration minimization using the ACSR scheme, by disturbance-rejection approach. For this multi-input/multi-output control problem, the controller is obtained by employing four-block representation and doubly coprime factorization theory.[21]

3) Evaluate the efficiency of the controller with the full-order model.

4) Study the influence of sensor location on the efficiency of the closed-loop vibration control scheme.

II. Mathematical Formulation

The presentation of the mathematical formulation is divided into two parts, with each part addressing a specific aspect. They are 1) equations of motion of the coupled gearbox–fuselage system and 2) design of closed-loop control law. A brief description of these items are presented next. The details of the formulation may be found in Refs. 22 and 23.

A. Equations of Motion and Decoupling into Controllable and Uncontrollable Modes

For the purpose of order reduction and closed-loop control of vibration in helicopter fuselages, a simplified dynamic model of the coupled rotor–gearbox–fuselage systems shown in Fig. 2, is considered. The gearbox is supported on the top of the fuselage at four nodes. Rotor blade dynamics are not included. However, the vibratory rotor loads are assumed to be acting at the top of the gearbox. The gearbox support is represented as a linear spring, a viscous damper, and an active force generator for vibration minimization. Note that this dynamic model represents an ACSR type of vibration minimization scheme adopted in helicopters.[7–12,14,15] Several simplifying assumptions have been made in formulating the equations of motion:

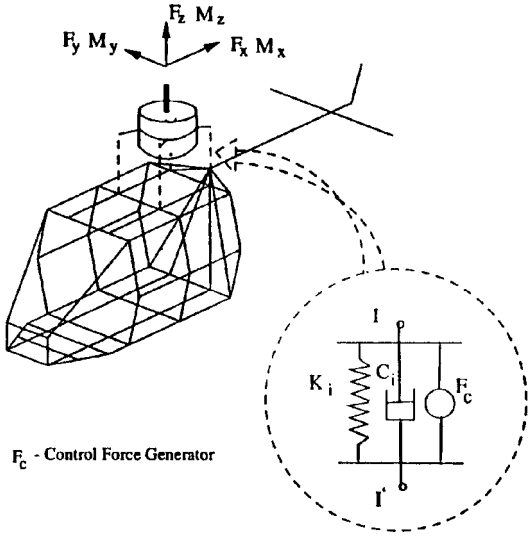

Fig. 2 Coupled gearbox–fuselage dynamic model.

1) The gearbox is assumed to be rigid and has only vertical translation, pitch, and roll degrees of freedom.

2) The fuselage is assumed to be undergoing rigid-body vertical translation and pitch and roll motions, as well as flexible deformation due to elastic modes.

3) The rigid body motions of the fuselage and gearbox are assumed to be small.

4) The products of inertia of the gearbox and fuselage are assumed to be zero.

5) The gearbox supports are assumed to be uniaxial members, providing forces only in the z direction.

The equations of motion of the coupled gearbox–fuselage system can be grouped into three sets. Set I corresponds to rigid-body equations of motion of the gearbox, set II presents the rigid-body equations of the fuselage, and set III represents the equations of motion of the elastic modes of the fuselage. The first 20 flexible modes of the fuselage have been considered in the formulation and analysis of the problem. These elastic modes have been obtained from an eigenanalysis of a three-dimensional finite element model of the fuselage, shown in Fig. 2. The details of the formulation of the equations are given in Ref. 22. The equations of motion of the coupled gearbox–fuselage system can be written in state-space form as

$$\{\dot{q}\} = [A_f]\{q\} + [B_w]\{w\} + [B_u]\{u\}$$

$$\{z\} = [C_z]\{q\}, \qquad \{y\} = [C_y]\{q\} \tag{1}$$

where $\{q\}$ is the state vector of the modal degrees of freedom, $\{w\}$ is the vibratory hub load (or external disturbance) whose effect on the fuselage is to be minimized, $\{u\}$ is actuator force (or control forces) acting at four locations at the top of the fuselage, $\{z\}$ is the output vector representing the response of the structure at various locations, and $\{y\}$ is the response at preselected sensor locations that are used for feedback to obtain the control forces. The size of the state vector is 52×1, corresponding to 3 rigid-body modes of the gearbox plus 3 rigid-body modes of the fuselage plus 20 flexible modes of the fuselage.

In Eq. (1), all of the rigid-body modes and flexible modes are highly coupled. Note that the effect of control forces on rigid-body modes is very weak, that is, from a control viewpoint the rigid-body modes are weakly controllable by the actuator control inputs. Hence, there are difficulties in obtaining a suitable control law for the model given in Eq. (1). The practical difficulties arise due to ill conditioning while computing the grammians, leading to very high value of gains in the resultant control laws.[24] A practical way of avoiding these difficulties is to separate the rigid-body modes from the other flexible modes before proceeding further toward designing the control law. This appears to have received little attention in the literature on vibration control of helicopter fuselages. The decoupling of modes into uncontrollable rigid-body modes and controllable flexible modes is carried out by the following step-by-step mathematical procedure.

1) Find a transformation $\bar{T}$ of the state space as $\{q\} = \bar{T}\{\tilde{q}\}$ to convert Eq. (1) to the form

$$\{\dot{\tilde{q}}\} = \begin{bmatrix} A_1 & 0 \\ 0 & A_2 \end{bmatrix}\{\tilde{q}\} + \begin{bmatrix} B_{w1} \\ B_{w2} \end{bmatrix}\{f\} + \begin{bmatrix} B_{u1} \\ B_{u2} \end{bmatrix}\{u\}$$

$$\{z\} = C_z\bar{T}\{\tilde{q}\}, \qquad \{y\} = C_y\bar{T}\{\tilde{q}\}$$

where A_2 is a 6×6 matrix whose eigenvalues (equal to zero) correspond to the rigid-body modes of the system. The details of formulating matrix $\bar{T}$ may be found in Ref. 23.

2) Partition $\{\tilde{q}\}$ as $[\{x_1\}\ \{x_2\}]^T$, where $\{x_2\}$ denotes the last six state variable corresponding to the rigid-body modes. Similarly partition $C_y\bar{T}$ and $C_z\bar{T}$ as $[C_{y1}\ \ C_{y2}]$ and $[C_{z1}\ \ C_{z2}]$, where C_{y2} and C_{z2} are the submatrices containing the last six columns of $C_y\bar{T}$ and $C_z\bar{T}$, respectively.

3) Express the model pertaining to the flexible (controllable) part of the dynamics as

$$\{\dot{x}_1\} = A_1\{x_1\} + B_{w1}\{f\} + B_{u1}\{u\}$$

$$\{z\} = C_{z1}\{x_1\}, \qquad \{y\} = C_{y1}\{x_1\} \tag{2}$$

Note that output vector $\{y\}$ and measurement vector $\{z\}$ in Eq. (2) contain only the effects due to the flexible (or controllable) part of the dynamics of the system. The size of the model given in Eq. (2) is 46th order, which is still very high from the point of view of the control design problem. In addition all of the states of this model will have different levels of controllability and observability. Hence, it is desirable to reduce the order of this model by eliminating weakly controllable and observable states (note that here weak or strong is only relative) in comparison to other states. A balanced-realization-based order reduction is applied to Eq. (2) to reduce the size of the problem. The details of the procedure can be found in Refs. 17, 19, and 20; the implementation details are given in Ref. 23.

B. Control Law for Disturbance Rejection

When the procedure described in Refs. 17, 19 and 20 is followed, a suitable transformation T for balanced realization is formulated. With the substitution of transformation $\{x_1\} = T^{-1}\{x_b\}$ and the premultiplication by T, Eq. (2) is transformed into a balanced-realization form, which is given by

$$\{\dot{x}_b\} = A_b\{x_b\} + B_{w1b}\{w\} + B_{u1b}\{u\}$$

$$\{z\} = C_{z1b}\{x_b\}, \qquad \{y\} = C_{y1b}\{x_b\} \tag{3}$$

where $A_b = TA_1T^{-1}$, $B_{w1b} = TB_{w1}$, $B_{u1b} = TB_{u1}$, $C_{z1b} = C_{z1}T^{-1}$, and $C_{y1b} = C_{y1}T^{-1}$.

From the Hankel singular values of the grammians in balanced space, weakly controllable and observable states are identified and deleted from Eq. (3); thus, a reduced-order model of the system is obtained. In the present problem, the 46 Hankel singular values corresponding to the 46 states are found to be in the range 0.5–0.002. The choice of the exact number of states to be deleted is arbitrary. However, one can use the error between the transfer functions of the original and the reduced system as a reference parameter. In the present study the criterion used for reducing the order of the system is based on stability constraint, that is, the controller designed for the reduced-order system must ensure closed-loop stability when incorporated in the full-order original system. The reduced-order model can be symbolically written as

$$\{\dot{x}\} = A\{x\} + B_1\{w\} + B_2\{u\}$$

$$\{z\} = C_1\{x\}, \qquad \{y\} = C_2\{x\} \tag{4}$$

where $\{x\}$, $\{w\}$, $\{u\}$, $\{z\}$, and $\{y\}$ are the reduced-order state vector, disturbance input, control inputs, measured output, and measurements for feedback control, respectively. For the present problem of vibration minimization in a helicopter fuselage, $\{z\}$ are the vibratory levels, at preselected optimal (or arbitrary) sensor locations, to be minimized. In the present study, the measurement quantity $\{y\}$ used for feedback is assumed to be same as $\{z\}$. Hence, in Eq. (7), one has $C_1 = C_2$. When the Laplace transform of Eq. (4) is taken and zero initial conditions are assumed, the standard four-block representation of Eq. (4) can be written as

$$\begin{bmatrix} \hat{z} \\ \hat{y} \end{bmatrix} = \begin{bmatrix} \hat{P}_1 & \hat{P}_2 \\ \hat{P}_3 & \hat{P}_4 \end{bmatrix} \begin{bmatrix} \hat{w} \\ \hat{u} \end{bmatrix} \tag{5}$$

where the variables with a caret are the Laplace transforms of the corresponding time-domain quantities. For the present case, one has

$$\hat{P}_1 = C_1(sI - A)^{-1}B_1 \tag{6}$$

$$\hat{P}_2 = C_1(sI - A)^{-1}B_2 \tag{7}$$

$$\hat{P}_3 = C_2(sI - A)^{-1}B_1 \tag{8}$$

$$\hat{P}_4 = C_2(sI - A)^{-1}B_2 \tag{9}$$

With the preceding four-block representation of the reduced-order system, the vibration minimization problem is cast as follows: Design a closed-loop controller with transfer function K such that the effect of the external disturbance $\{w\}$ is asymptotically reduced to zero in the output $\{z\}$ while providing closed-loop stability, that is, determine a controller $\hat{u} = \hat{K}\hat{y}$ such that the closed-loop system with this controller is stable. The controller is obtained as a solution of the following disturbance rejection problem.

The closed-loop transfer function between input $\{w\}$ and output $\{z\}$ can be expressed as

$$\hat{z} = \left[\hat{P}_1 + \hat{P}_2\hat{K}(I - \hat{P}_4\hat{K})^{-1}\hat{P}_3\right]\hat{w} \tag{10}$$

$$\hat{z} = T_{zw}\hat{w} \tag{11}$$

The idea of disturbance rejection requires satisfying the condition that the transfer function T_{zw} has a zero at the frequency of the external disturbance $\{w\}$, which is $\omega_0 = \text{NB/rev}$, that is, $T_{zw}(j\omega_0) = 0$. Because T_{zw} is a nonlinear function of the closed-loop gain $\hat{K}$, solving the preceding equation for $\hat{K}$ is difficult.

A solution to this problem can be found by using the factorization theory of feedback system synthesis.[21] In this approach, the set of all controllers that provide closed-loop stability is given by the following equivalent formulas

$$\hat{K} = (Y - M\bar{Q})(X - N\bar{Q})^{-1} \quad \text{or} \quad \hat{K} = (\tilde{X} - \bar{Q}\tilde{N})^{-1}(\tilde{Y} - \bar{Q}\tilde{M}) \tag{12}$$

where, N, M, $\tilde{N}$, and $\tilde{M}$ are stable transfer function matrices obtained from a doubly coprime factorization of P_4; X, Y, $\tilde{X}$, and $\tilde{Y}$ satisfy the Bezout identity; and $\bar{Q}$ is an arbitrary stable proper transfer matrix of conformable size. The advantage of this formula is that, on substitution in Eq. (10), the transfer matrix T_{zw} of the stable closed-loop system can be expressed as

$$T_{zw} = T_1 - T_2\bar{Q}T_3 \tag{13}$$

The details of the formulation and expressions for T_1, T_2, and T_3 can be found in Ref. 23. In the modified form given by Eq. (13), transfer matrix T_{zw} is linearly related to matrix $\bar{Q}$. Therefore, the requirement of asymptotic disturbance rejection on vibration minimization is satisfied by finding a stable transfer function $\bar{Q}$ such that

$$T_1(\pm j\omega_0) - T_2(\pm j\omega_0)\bar{Q}(\pm j\omega_0)T_3(\pm j\omega_0) = 0 \tag{14}$$

Any transfer matrix $\bar{Q}(s)$ that is stable, proper, and satisfies the preceding equation provides a closed-loop controller $\hat{K}$ that meets the requirement of disturbance rejection at the specified frequency ω_0.

In the present study, the matrix $\bar{Q}$ is evaluated by representing each element, for example, ijth element, of $\bar{Q}$ by a second-order stable transfer function of the form

$$\bar{Q}_{ij} = \frac{s^2 + as + b}{(s+1)^2} \tag{15}$$

The two unknown quantities a and b are solved by first substituting $s = \pm j\omega_0$ in $\bar{Q}$ and formulating two sets of algebraic equations by equating each element of the matrix Eq. (14) to zero, separately for $+j\omega_0$ and $-j\omega_0$.

III. Results and Discussion

With the use of the dynamic model of the coupled gearbox–flexible fuselage system shown in Fig. 2, an order reduction based on the balanced-realization approach is performed. Then a closed-loop controller is designed using the reduced-order model. The controller design is based on the disturbance-rejection scheme, using doubly coprime stable factorization theory, described in Sec. II.B. The output measurements used for the controller design are the vibratory levels at preselected sensor locations. The effectiveness of

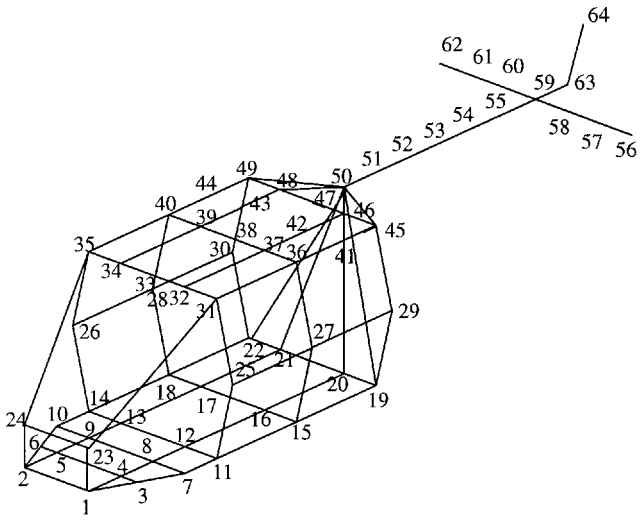

Fig. 3 Finite element model of helicopter fuselage.

the controller is evaluated by performing the vibratory response of the full-order system incorporating the closed-loop controller designed for the reduced-order model. In addition, the influence of sensor locations on the performance of closed-loop vibration control is studied. A detailed description of the dynamic model and the results of the studies are presented in the following paragraphs.

Figure 3 shows the schematic of a finite element model of the helicopter fuselage. The length, height, and width of the model are 8.25, 2, and 3 m, respectively. The fuselage is 4 m long, with a width of 2.5 m and a height of 1.5 m. The tail boom length is 4.25 m, and the span of the horizontal stabilizer is 3 m. Lumped masses representing two engines, a tail gearbox, and two end plates are also attached to the structure at appropriate nodes. The total number of nodes and the degrees of freedom are 64 and 356, respectively. The details of the structural properties, node locations, and other data are given in Ref. 25. It was shown in Ref. 25 that the undamped natural frequencies and mode shapes of this model are similar to those of a realistic helicopter.

When it is assumed that the main rotor system consists of four blades, the vibratory hub loads will have a nondimensional excitation frequency of 4/rev. For the fuselage model, the nondimensional frequency of the 20th flexible mode is 6.41 (Ref. 25), which is 50% more than the excitation frequency (4/rev) of the hub loads. The coupled gearbox–fuselage model, shown in Fig. 2, has the gearbox mounted on the roof of the fuselage at the four nodes (39, 48, 46, and 37). The vibration analysis is performed by applying vibratory loads at the top of the gearbox. Because the vibratory load in the vertical direction is more predominant, without loss of generality, it is assumed that the sensors measure only the vertical z component of fuselage vibration. The total number of degrees of freedom considered in the analysis is 26. These include 3 rigid-body modes of the gearbox (pitch, roll, and heave) and 3 rigid-body modes and 20 flexible modes of the fuselage. In state-space form, the order of the system is 52, and this model is treated as the full-order system in this study. The data used for the analysis are given in Table 1.

A. Sensor Locations

A key aspect in vibration control is the choice of sensor locations for measurement of vibratory levels in the fuselage and for feedback in the closed-loop control scheme. In Ref. 12, following a mathematical procedure involving the Fisher information matrix and effective independence distribution vector, 23 optimal sensor locations were identified. These optimal sensor locations are shown by node numbers in Fig. 4, taken from Ref. 12. It was shown in Ref. 12 that irrespective of the excitation frequency, these optimally selected sensors measure high levels of vibration. When a four-bladed rotor system is considered and a 4/rev vibratory hub force in the z direction is assumed, the baseline vibratory levels in the fuselage at all of the nodes are shown in Fig. 5. Node number 0 refers to the gearbox c.g. location. The arrows in Fig. 5 indicate the locations

Table 1 Data used for vibration and control analysis

Parameter	Value
Reference quantities for nondimensionalization	
m_b, kg	65
R, m	6
Ω, rad/s	32
Nondimensional quantities	
K_i	60.01
C_i	0.033
m_F	33.846
m_{GB}	4.615
I_{xxF}	0.6838
I_{yyF}	2.735
$I_{xx\mathrm{GB}} = I_{yy\mathrm{GB}}$	0.0171
$F_z/m_b\Omega^2 R$	0.0001
Location of center of mass of fuselage from origin[a]	
x	0.5632
y	0
z	0.0833
Location of center of mass of gearbox from origin[a]	
x	0.5632
y	0
z	0.3333
Structural damping of fuselage elastic modes	
β_F	0.005

[a] At nose of the fuselage.

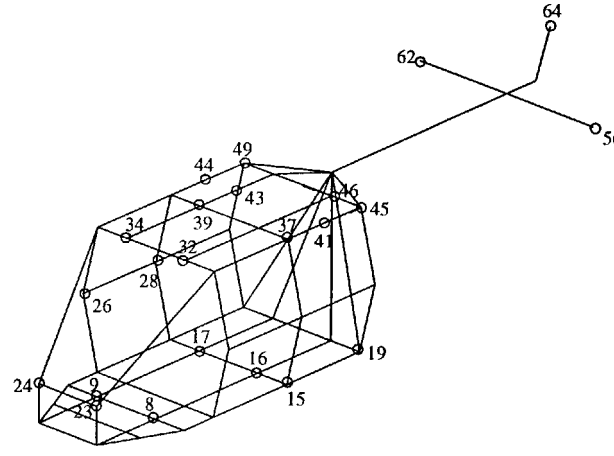

Fig. 4 Optimal sensor locations (indicated by node numbers).

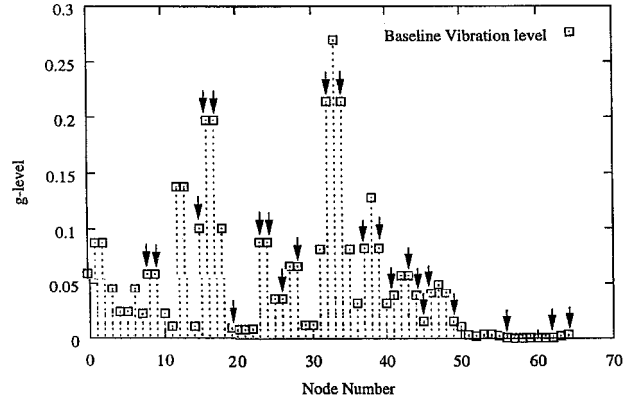

Fig. 5 Baseline vibratory levels for 4/rev excitation: arrows indicate optimal sensor locations, node 0 refers to gearbox c.g. location.

of 23 optimal sensors. The peak vibratory response occurs at node 33. Although, optimal selection procedure does not identify node 33, there are two sensors at node locations 32 and 34 measuring the second highest level of response.

In the present study, three different sets of five sensor locations are considered for order reduction and closed-loop vibration control. The reason for choosing five sensors is to provide redundancy for the closed-loop control problem in determining the control forces

for the four control actuators. The three sets of sensors locations are as follows: Set I has sensors at node locations 8, 17, 23, 34, and 39 (these locations are selected from the optimal set of 23 sensor locations providing high levels of baseline vibratory response, as shown in Fig. 5). Set II consists of sensors at node locations 12, 16, 32, 33, and 38 (these locations represent the locations corresponding to five maximum vibratory response levels, as shown in Fig. 5). Set III has the sensors at 6, 20, 28, 44, and 64 (these locations correspond to the low vibratory response locations, as can be seen as Fig. 5).

B. Reduced-Order Model

The dynamics of the coupled gearbox–flexible fuselage system is represented by a 52nd-order model. The full-order system (52nd order) is decomposed into controllable (46th order) and uncontrollable (6th order) subsystems, by performing a transformation of states to obtain a block diagonal form of the system matrix, as described in Sec. II.A. The eigenvalues corresponding to the block diagonal form of the controllable part (46th order) are given in Table 2. The uncontrollable rigid-body modes having zero eigenvalues (sixth order) correspond to the other block diagonal matrix.

Note that the reduced-order model depends on measurement matrix C, which is related to sensor locations. For conciseness, only those results pertaining to sensor set I are presented here. Table 3 presents the Hankel singular values of the grammians in balanced space of the controllable 46th-order system, arranged in descending order. The singular values vary in the range 0.5–0.002, indicating the effectiveness of the states in the input–output relation. Initially (by trial), the system was truncated to a 10th order model. This 10th order model provided a good approximation of the frequency response of the original system. However, the controller designed for the 10th-order reduced model could not effectively stabilize the full-order system. The reason could be attributed to the spillover instability due to the excitation of the truncated or residual modes.[24] Then the size of the reduced-order model is increased one order at a time until closed-loop stability of the full-order system is ensured. An 18th order model is found to provide both a good approximation to the frequency response and a stable controller for the full-order system. For comparison, the frequency response (both gain and phase) of the 18th order reduced model (plus 6 uncontrollable rigid-body modes) with that of the full-order system (46 controllable plus 6 uncontrollable states) at node 23 is shown in Fig. 6. It is evident that the frequency response of the reduced-order model matches very well that of the full-order system up to the frequency 5/rev. A similar good correlation was also found for the frequency response

Table 2 Eigenvalues of the 46th-order flexible part of system dynamics

No.	Eigenvalues
1	$-0.08875 \pm i17.29791$
2	$-0.02800 \pm i12.30483$
3	$-0.02796 \pm i11.93083$
4	$-0.03475 \pm i7.05896$
5	$-0.03070 \pm i6.13030$
6	$-0.03189 \pm i5.82441$
7	$-0.03291 \pm i5.53105$
8	$-0.02646 \pm i5.44131$
9	$-0.02529 \pm i4.92342$
10	$-0.02488 \pm i4.79801$
11	$-0.02422 \pm i4.76666$
12	$-0.02235 \pm i4.42907$
13	$-0.02291 \pm i4.39552$
14	$-0.02381 \pm i3.70094$
15	$-0.01984 \pm i3.47435$
16	$-0.01526 \pm i3.05898$
17	$-0.01329 \pm i2.63113$
18	$-0.01309 \pm i2.60198$
19	$-0.01239 \pm i2.38375$
20	$-0.01463 \pm i2.24567$
21	$-0.01092 \pm i2.19632$
22	$-0.00408 \pm i0.81457$
23	$-0.00484 \pm i0.66367$

Table 3 Hankel singular values of the grammians in balanced state

No.	Singular values	No.	Singular values
1	0.50020	24	0.12181
2	0.49787	25	0.09296
3	0.39793	26	0.09163
4	0.39404	27	0.08658
5	0.35759	28	0.08566
6	0.35421	29	0.07624
7	0.34479	30	0.07548
8	0.34131	31	0.05103
9	0.29946	32	0.05027
10	0.29678	33	0.04351
11	0.29174	34	0.04332
12	0.29043	35	0.03378
13	0.25460	36	0.03370
14	0.25195	37	0.02160
15	0.22469	38	0.02147
16	0.22362	39	0.01791
17	0.17680	40	0.01772
18	0.17487	41	0.01556
19	0.12997	42	0.01543
20	0.12909	43	0.00224
21	0.12543	44	0.00222
22	0.12419	45	0.00213
23	0.12303	46	0.00211

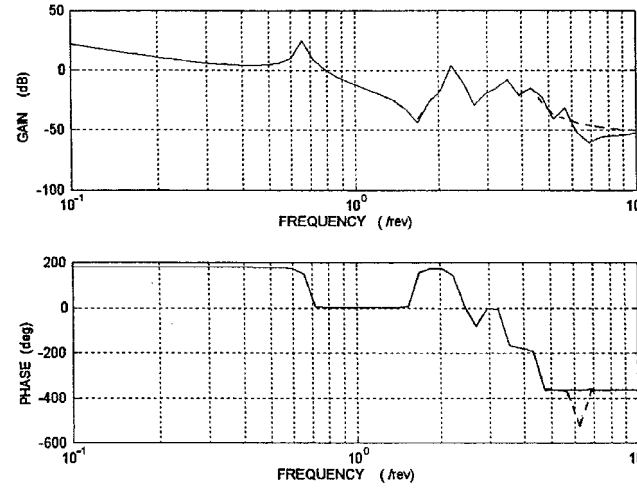

Node 23

Fig. 6 Comparison of frequency response of full- and reduced-order models: - - - -, reduced-order system and ——, full-order system.

at other sensor locations, namely, nodes 8, 17, 34, and 39. Considering that the controller will be designed to reduce the fuselage vibration at the excitation frequency of 4/rev, it can be stated that in the frequency range of interest the 18th order reduced model (plus 6 rigid-body uncontrollable modes) is an excellent approximation to the 52nd-order full model.

C. Closed-Loop Vibration Control

When the reduced-order model is used and the disturbance-rejection approach based on factorization theory is followed, a controller is designed to minimize the vibration in the fuselage. This controller is incorporated in the feedback loop of the full-order system, and the vibratory level of the fuselage is calculated at all of the nodes. The study is carried out for the three different sets of sensor locations. (Note that the controller is designed using only the reduced-order model of the controllable states.) The results corresponding to these cases are presented in the following subsections.

1. Optimal Sensor Locations (Set I: Nodes 8, 17, 23, 34, and 39)

The comparison of baseline and controlled vibratory levels at all of the 64 nodes is shown in Fig. 7. The arrows in Fig. 7 indicate the

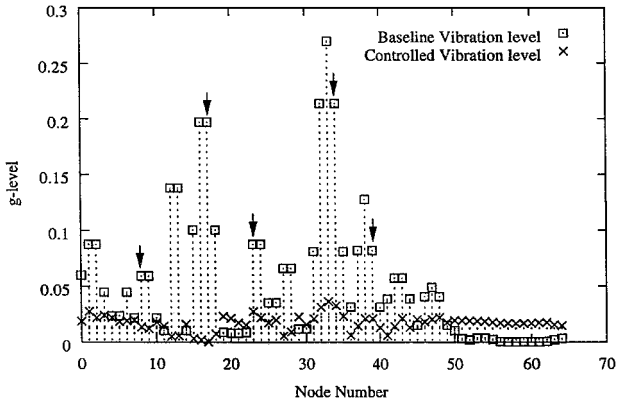

Fig. 7 Comparison of baseline and closed-loop controlled vibratory levels; set I: 8, 17, 23, 34, and 39, sensor locations indicated by arrows, node 0 refers to gearbox c.g. location.

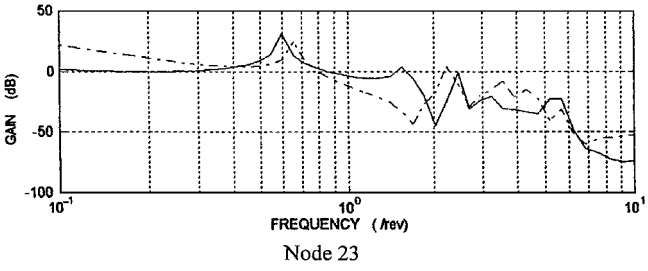

Fig. 8 Frequency response of uncontrolled and closed-loop controlled full system: –·–, uncontrolled system and ——, controlled system.

locations of the five sensors (set I). Node number 0 indicates the c.g. of the gearbox. For the baseline configuration, the peak vibratory level is 0.27 *g* at node location 33, and the lowest level is at node 57 with a value of 0.00017 *g*. With closed-loop control, the peak vibratory level is reduced to 0.036 *g* at node 33. Although, closed-loop control reduces the vibratory levels in the fuselage substantially, there is an increase in vibratory response at the tail portion. For example, at node 64, the vibratory level is increased from the baseline value of 0.0032 *g* to 0.0145 *g*. The reason for this increase can be attributed to not having a sensor in the tail portion. Note that with closed-loop control, the vibratory level in the gearbox c.g. (node 0) is reduced from a baseline value of 0.06–0.019 *g*. This observation seems to be contrary to the vibration reduction schemes using open control,[12,14] where a reduction in fuselage vibration increases the vibratory level in the gearbox (or hub). In the present case of the closed-loop control scheme, the vibratory levels at both fuselage and gearbox are reduced simultaneously.

The frequency response of the gain for the uncontrolled and the controlled full-order system at the sensor located at node 23 is shown in Fig. 8. It can be seen that the controller is effective in reducing the vibration not only at desired frequency of 4/rev but also in the neighborhood of the desired frequency, indicating the robustness of the control scheme.

2. Choice of Highest Vibration Nodes (Set II: Nodes 12, 16, 32, 33, and 38)

For closed-loop vibration control, another set of five arbitrary sensor locations measuring the five highest baseline vibratory levels has been considered. These node locations are not part of the optimal set as per Ref. 12, except nodes 16 and 32. For this set of sensor locations, first a reduced-order model is obtained. It is found that a 20th-order model is needed to satisfy the condition of closed-loop stability.

A comparison of the baseline and controlled vibratory response is shown in Fig. 9. With closed-loop control, the maximum vibratory response is found to be 0.033 *g* at node location 17, whereas the peak response for the baseline configuration is 0.27 *g* at node 33. The tail portion experiences an increase in vibratory levels for closed-loop control. For example, at node 64, the vibratory level increases from

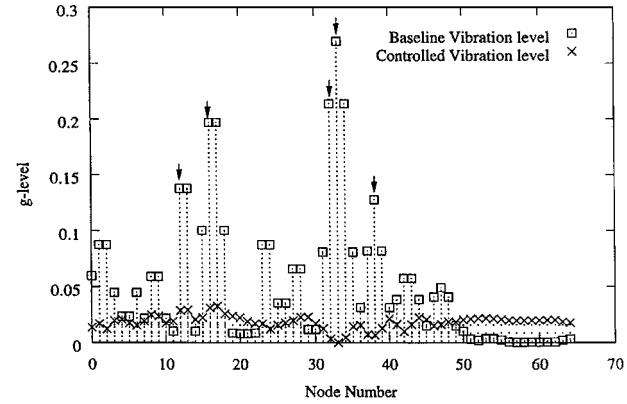

Fig. 9 Comparison of baseline and closed-loop controlled vibratory levels; set II: 12, 16, 32, 33, and 38, sensor locations indicated by arrows, node 0 refers to gearbox c.g. location.

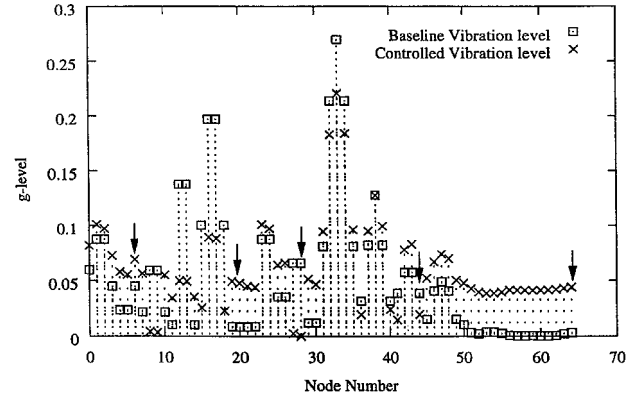

Fig. 10 Comparison of baseline and closed-loop controlled vibratory levels; set III: 6, 20, 28, 44, and 64, sensor locations indicated by arrows, node 0 refers to gearbox c.g. location.

a baseline value of 0.0032–0.018 *g*. At gearbox c.g. (node 0), there is a reduction in vibration from a baseline level of 0.06–0.014 *g*.

When the results corresponding to optimal set of sensor locations (set I) and the set of sensor locations measuring the highest vibratory levels (set II) are compared, it can be concluded that the vibration reduction with the optimal set is as efficient as the other set measuring highest vibratory levels, even though the optimal set does not provide a sensor at node 33 experiencing highest baseline vibratory level. This result validates the mathematical procedure of identifying the optimal sensor locations for vibration measurement presented in Ref. 12.

3. Choice of Low Vibration Notes (Set III: Nodes 6, 20, 28, 44, and 64)

To evaluate the influence of sensor locations on closed-loop vibration control, a set of five sensor locations measuring low (not the lowest) vibratory levels are chosen. For this choice of sensor locations, the reduced-order model is found to be of size 30, which is very high compared to the other two cases.

A comparison of baseline and controlled vibratory response is shown in Fig. 10. With closed-loop control, the maximum vibratory level is found to be 0.22 *g*, which is close to the baseline level of 0.26 *g*. In addition, it can be seen that, with closed-loop control, the level of vibration is increased at the majority of the nodes. The reason for this inefficiency may be attributed to the formulation of the control law based on an incorrect picture of the true vibratory levels in the fuselage, leading to inaccurate control forces.

This result clearly indicates that the choice of sensor locations is very important for order-reduction and vibration control schemes.

4. Control Forces

The magnitudes and phase angles of the control forces in the four actuators for closed-loop vibration minimization have been evaluated for the three cases considered. Table 4 presents the magnitude

Table 4 Magnitude and phase angle of control forces

Control force	Node no.	Five optimal sensor locations	Five high-vibration nodes	Five low-vibration nodes
Magnitude $(1.0E+03)$	39	1.9218	1.1754	0.04305
	48	2.9892	1.4224	0.03673
	46	0.8335	1.4095	0.03047
	37	0.5604	0.9981	0.08552
Phase angle, deg	39	−154.2	−150.5	−3.9
	48	−154.5	−137.1	−2.0
	46	52.5	70.4	7.3
	37	45.8	63.3	0.1

and phase angle of the control forces corresponding to the three cases. For vibration reduction with sensor sets I and II, the control forces and the phase angles are found to be of the same order, whereas for sensor set III, the magnitudes and phase angles are completely different, resulting in inefficient vibration control.

IV. Conclusions

Application of balanced-realization-based order reduction has been carried out to obtain a reduced-order model for a coupled gearbox–flexible fuselage dynamic system. By the use of the reduced-order model, a closed-loop controller is developed using a disturbance-rejection approach based on internal model principle and stable coprime factorization theory. The most important conclusions of this study are summarized as follows.

A 46th-order controllable subsystem of the coupled gearbox–flexible fuselage model is reduced to an 18th-order model, using the balanced-realization approach. The frequency response of the reduced model closely matches the full-order system in the frequency range of interest.

The controller designed for the reduced-order model provided a substantial reduction in fuselage vibratory levels. The controller is found to provide vibration reduction not only at the desired frequency but also in the neighborhood of the desired frequency. In addition, contrary to open-loop control, in this study it is observed that closed-loop control reduces not only the fuselage vibration but also the vibratory level in the gearbox.

The set of five sensor locations (measuring high vibratory levels) chosen from the optimal set provides vibration reduction in the fuselage that is as efficient as the set of five sensors (not all pertaining to the optimal set) measuring the highest vibratory levels. This result validates the mathematical procedure of identifying the optimal sensor locations, followed in Ref. 12. The controller designed for the set of five sensors measuring low levels of vibration is very inefficient, and it is shown to increase the fuselage vibration at several locations. This observation substantiates the importance of choice of sensor locations for vibration control.

Acknowledgment

The authors wish to acknowledge the financial support from the Structures Panel of the Aeronautics Research and Development Board, India.

References

[1]Crews, S. T., "Rotorcraft Vibration Criteria: A New Perspective," *Proceedings of the 43rd Annual Forum of the American Helicopter Society*, American Helicopter Society, Alexandria, VA, 1987, pp. 991–998.

[2]Reichert, G., "Helicopter Vibration Control-A Survey," *Vertica*, Vol. 5, No. 1, 1981, pp. 1–20.

[3]Loewy, R. G., "Helicopter Vibrations: A Technological Perspective," *Journal of the American Helicopter Society*, Vol. 29, No. 4, 1984, pp. 4–30.

[4]Kvaternik, R. G., Bartlett, F. D., Jr., and Cline, J. H., "A Summary of Recent NASA/ARMY Contributions to Rotorcraft Vibrations and Structural Dynamics Technology," *NASA/Army Rotorcraft Technology*, CP-2495, NASA, 1988, pp. 71–179.

[5]Huber, H., "Parametric Trends and Optimization-Preliminary Selection of Configuration—Prototype Design and Manufacture," *Helicopter Aerodynamics and Dynamics*, AGARD LS-63, 1973, pp. 8.1–8.55.

[6]Stoppel, J., and Degener, M., "Investigations of Helicopter Structural Dynamics and a Comparison with Ground Vibration Tests," *Journal of the American Helicopter Society*, Vol. 27, No. 2, 1982, pp. 34–42.

[7]Rottmayr, H., Popp., W., and Mehlhose, R., "Application of Modern Vibration Control Techniques on EC135 and Future Trends," *Proceedings of the 23rd European Rotorcraft Forum*, German Society for Aeronautics and Astronautics, Bonn, 1997, pp. 51.1–51.17.

[8]Friedmann, P. P., and Millott, T. A., "Vibration Reduction in Rotorcraft Using Active Control: A Comparison of Various Approaches," *Journal of Guidance, Control, and Dynamics*, Vol. 18, No. 4, 1995, pp. 664–673.

[9]King, S. P., and Staple, A. E., "Minimization of Vibration Through Active Control of Structural Response," *Rotorcraft Design Operations*, CP-423, AGARD, 1986, pp. 14.1–14.13.

[10]Staple, A. E., "An Evaluation of Active Control of Structural Response as a Means of Reducing Helicopter Vibration," *Proceedings of the 15th European Rotorcraft Forum*, Nederlandse Vereniging voor Luchtvaarttechniek, Amsterdam, 1989, pp. 3–17.

[11]Welsh, W., Fredrickson, C., Rauch, C., and Lyndon, I., "Flight Test of an Active Vibration Control System on the UH-60 Black Hawk Helicopter," *Proceedings of the 51st Annual Forum of the American Helicopter Society*, American Helicopter Society, Alexandria, VA, 1995, pp. 393–402.

[12]Venkatesan, C., and Udayasankar, A., "Selection of Sensor Locations for Active Vibration Control of Helicopter Fuselages," *Journal of Aircraft*, Vol. 36, No. 2, 1999, pp. 434–442.

[13]Kammer, D. C., "Sensor Placement for On-Orbit Modal Identification and Correlation of Large Space Structures," *Journal of Guidance, Control, and Dynamics*, Vol. 14, No. 2, 1991, pp. 251–259.

[14]Chiu, T., and Friedmann, P. P., "ACSR System for Vibration Suppression in Coupled Helicopter Rotor/Flexible Fuselage Model," *Proceedings of the AIAA/ASME/ASCE/AHS/ASC 37th Structures, Structural Dynamics, and Materials Conference*, AIAA, Reston, VA, 1996, pp. 1972–1990.

[15]Reichert, G., and Huber, H., "Active Control of Helicopter Vibration," *Proceedings of the 4th Workshop on Dynamics and Aeroelastic Stability Modelling of Rotorcraft Systems*, Univ. of Maryland, College Park, MD, 1991, pp. 1–20.

[16]Francis, B. A., and Wonham, W. M., "The Internal Model Principal of Control Theory," *Automatica*, Vol. 12, No. 5, 1976, pp. 457–465.

[17]Moore, B. C., "Principal Component Analysis in Linear Systems: Controllability, Observability, and Model Reduction," *IEEE Transactions on Automatic Control*, Vol. AC-26, No. 1, 1981, pp. 17–32.

[18]Gawronski, W., and Williams, T., "Model Reduction for Flexible Space Structures," *Journal of Guidance, Control, and Dynamics*, Vol. 14, No. 1, 1991, pp. 68–76.

[19]Pernebo, L., and Silverman, L. M., "Model Reduction via Balanced State Space Representations," *IEEE Transactions on Automatic Control*, Vol. AC-27, No. 2, 1982, pp. 382–387.

[20]Inman, D. J., *Vibration with Control, Measurement, and Stability*, Prentice–Hall, Upper Saddle River, NJ, 1989, pp. 163–167.

[21]Francis, B. A., *A Course in H_∞ Control Theory*, Lecture Notes in Control and Information Sciences, No. 88, Springer-Verlag, Berlin, 1986, pp. 22–47.

[22]Udayasankar, A., "Choice of Sensor Locations and Vibration Control in Flexible Fuselage System," M.Tech Thesis, Dept. of Aerospace Engineering, Indian Inst. of Technology, Kanpur, India, March 1997.

[23]Mathews, A., "Order Reduction and Vibration Minimization in Helicopter Fuselage," M.Tech Thesis, Dept. of Electrical Engineering, Indian Inst. of Technology, Kanpur, India, Oct. 1998.

[24]Balas, M. J., "Trends in Large Space Structure Control Theory: Fondest Hopes, Wildest Dreams," *IEEE Transactions of Automatic Control*, Vol. AC-27, No. 3, 1982, pp. 522–535.

[25]Mangalick, S., Venkatesan, C., and Kishore, N. N., "Formulation and Dynamic Analysis of a Helicopter Fuselage Model," Dept. of Aerospace Engineering, TR IITK/AE/ARDB/AVCH/826/95/01, Indian Inst. of Technology, Kanpur, India, 1995.